

Structural differences in Mg-doped InN – indication of polytypism

Z. Liliental-Weber^{*1}, M. E. Hawkrigde¹, X. Wang², and A. Yoshikawa³

¹ Materials Sciences Division, Lawrence Berkeley National Laboratory, 1 Cyclotron Road, Berkeley, CA 94720-8197, USA

² State Key Laboratory of Artificial Microstructure and Mesoscopic Physics, School of Physics, Peking University, Beijing 100871, China

³ Chiba University, Chiba 263-8522, Japan

Received 8 October 2009, revised 10 November 2009, accepted 10 November 2009

Published online 30 April 2010

Keywords InN, MBE, doping, dislocations, structure, TEM

* Corresponding author: e-mail Z_Liliental-Weber@lbl.gov

Transmission Electron Microscopy shows that the InN samples doped with either increasing or constant Mg concentration follow a cation or anion substrate polarity. In-polar samples change growth polarity when the Mg concentration is $>10^{19} \text{ cm}^{-3}$. N-polar samples have much higher density of planar defects than In-polar samples and their presence leads to a decrease in dislocation den-

sity. In the N-polar samples equally spaced planar defects are observed for Mg concentration $>10^{19} \text{ cm}^{-3}$. Three different polytypes (2H, 3C and 4H) were observed in this type of samples. A band of planar defects with thick layers of a cubic material (3C) is observed for Mg concentration $>10^{20} \text{ cm}^{-3}$. At this Mg concentration only n-type conductivity was reported earlier.

© 2010 WILEY-VCH Verlag GmbH & Co. KGaA, Weinheim

1 Introduction Among III-Nitrides InN was the least studied compound because obtaining high structural quality was difficult mainly due to low dissociation temperature and high equilibrium vapor pressure of Nitrogen and weak bonding of In and N [1]. However, alloying with GaN and AlN allows light emission from ultraviolet to red due to its narrow band gap [2], covering in this way the whole solar spectrum. This compound has a potential application in microelectronics, optoelectronics and solar cells [1,2].

In order to apply InN to devices one needs to be sure that p doping in this material is possible. While undoped InN films are always n-type, p-type doping is still difficult to achieve due to the unusual band structure of InN [3,4] and the presence of an electron accumulation layer [5]. Only recently was this electron accumulation layer overcome by using electrolyte-based capacitance-voltage (ECV) measurements [6,7] and a combination of Hall effect, photoluminescence and ECV analysis [8]. Mg doped InN thin films were confirmed to be p-type. However, there are only few reports on structural properties of this compound [9-11]. Detailed knowledge on the structural properties might lead to better understanding of electrical measurements and shed light on an earlier dispute of band gap of this compound [12].

In this paper the results of Transmission Electron Microscopy (TEM) studies will be presented on the structure of Mg doped InN layers grown by MBE.

2 Experimental Four samples doped with Mg will be described. All samples were grown by Molecular Beam Epitaxy (MBE) either on Ga-or N- GaN/c-Al₂O₃ substrates. The detailed growth procedure was described earlier [9,13,14]. The different growth polarities GaN substrates were used in order to obtain InN either with an anion or a cation growth polarity. Two samples were grown in opposite polarities with multilayers of InN:Mg, where each layer had an equal thickness but increased Mg concentration ($1 \times 10^{18} \text{ cm}^{-3}$, $5.6 \times 10^{18} \text{ cm}^{-3}$, $2.9 \times 10^{19} \text{ cm}^{-3}$ and $1.8 \times 10^{20} \text{ cm}^{-3}$) intersected by thin undoped layers leading to a total layer thickness of 2.2 μm . Two other samples were grown on identical substrates in different polarities with a constant Mg concentration of $6 \times 10^{18} \text{ cm}^{-3}$ and $3 \times 10^{19} \text{ cm}^{-3}$ and a thickness of 3.5 μm and 7.3 μm , respectively. As mentioned in earlier papers [9,13,14] different growth temperatures were used for growth on the substrates with different polarities. Different methods of transmission electron microscopy have been used to characterize these layers: classical methods for defect identification, lattice image for more in depth characterization of particular defect and Convergent Beam Electron Diffraction.

Report Documentation Page

Form Approved
OMB No. 0704-0188

Public reporting burden for the collection of information is estimated to average 1 hour per response, including the time for reviewing instructions, searching existing data sources, gathering and maintaining the data needed, and completing and reviewing the collection of information. Send comments regarding this burden estimate or any other aspect of this collection of information, including suggestions for reducing this burden, to Washington Headquarters Services, Directorate for Information Operations and Reports, 1215 Jefferson Davis Highway, Suite 1204, Arlington VA 22202-4302. Respondents should be aware that notwithstanding any other provision of law, no person shall be subject to a penalty for failing to comply with a collection of information if it does not display a currently valid OMB control number.

1. REPORT DATE OCT 2009		2. REPORT TYPE		3. DATES COVERED 00-00-2009 to 00-00-2009	
4. TITLE AND SUBTITLE Structural differences in Mg-doped InN - indication of polytypism				5a. CONTRACT NUMBER	
				5b. GRANT NUMBER	
				5c. PROGRAM ELEMENT NUMBER	
6. AUTHOR(S)				5d. PROJECT NUMBER	
				5e. TASK NUMBER	
				5f. WORK UNIT NUMBER	
7. PERFORMING ORGANIZATION NAME(S) AND ADDRESS(ES) Lawrence Berkeley National Laboratory, Materials Sciences Division, 1 Cyclotron Road, Berkeley, CA, 94720-8197				8. PERFORMING ORGANIZATION REPORT NUMBER	
9. SPONSORING/MONITORING AGENCY NAME(S) AND ADDRESS(ES)				10. SPONSOR/MONITOR'S ACRONYM(S)	
				11. SPONSOR/MONITOR'S REPORT NUMBER(S)	
12. DISTRIBUTION/AVAILABILITY STATEMENT Approved for public release; distribution unlimited					
13. SUPPLEMENTARY NOTES See also ADM002356. Presented at the International Conference on Nitride Semiconductors (8th) (ICNS8) Held in Jeju, Korea on October 18-23, 2009. Sponsored by AOARD.					
14. ABSTRACT					
15. SUBJECT TERMS					
16. SECURITY CLASSIFICATION OF:			17. LIMITATION OF ABSTRACT Same as Report (SAR)	18. NUMBER OF PAGES 4	19a. NAME OF RESPONSIBLE PERSON
a. REPORT unclassified	b. ABSTRACT unclassified	c. THIS PAGE unclassified			

tion (CBED) for determination of growth polarity of several areas of each sample.

3 TEM results CBED patterns were taken on four samples in different areas. These patterns show that the InN layers start to grow following the substrate polarity. For the sample with multilayers of InN:Mg CBED patterns indicate that InN layer started to grow with In-growth polarity following the Ga-polarity of a GaN substrate.

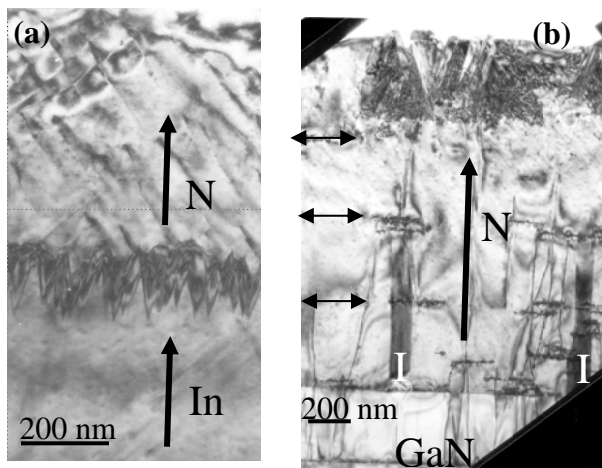


Figure 1 (a) An area of the InN sample with a zig-zag shape inversion boundary where the growth polarity changed from In polarity in the lower part to N-growth polarity in the upper part. (b) The entire layer of an InN sample grown with a N-polarity grown on N-polar GaN is presented. Each double-arrow indicates where Mg concentration is changing from $1 \times 10^{18} \text{ cm}^{-3}$ to $5.6 \times 10^{18} \text{ cm}^{-3}$ (the lowest one), then to $2.9 \times 10^{19} \text{ cm}^{-3}$ (central one), and to $1.8 \times 10^{20} \text{ cm}^{-3}$ (the upper one). Note the formation of twins in the top part of the layer and many planar defects arranged in a spacer layers when Mg concentration is rapidly changing. Two darker areas marked by "I" might be either imbedded inversion domains or areas with a different composition.

A drastic difference in structural perfection of the InN samples grown with different polarities was observed. The density of dislocations in this sample is as high as $3.6 \times 10^{10} \text{ cm}^{-2}$. When the thickness of the sample is about $1.7 \mu\text{m}$ growth polarity changed to N-polarity (Fig. 1a). This would suggest that Mg is floating to the sample surface and most probably reaches the concentration of about $5 \times 10^{19} \text{ cm}^{-3}$ at which point the growth polarity changes. At these conditions an inversion boundary with a continuous zig-zag (or V) shape was formed (Fig. 1a). This type of boundary was reported earlier for InN:Mg [9] and GaN:Mg [15] approximately for the same Mg concentration. Density of dislocations above this boundary was significantly reduced.

With a further increase of Mg concentration a layer approximately a 100 nm thick of densely distributed planar defects was formed leading to a very low dislocation density in the $0.2 \mu\text{m}$ of the subsurface area (Fig. 2a). Earlier studies on similar samples [8] show that an increase of Mg concentration above $1.8 \times 10^{20} \text{ cm}^{-3}$ using ECV measurements leads to a change from p-conductivity to n-type.

This concentration would be expected at the sample thickness where subsurface planar defects are formed, assuming Mg floatation to the sample surface.

The multilayer InN:Mg sample grown on N-polar GaN has N-growth polarity (Fig. 1b). This sample has much lower dislocation density already close to the interface with GaN. At the top part of the layer dislocation density did not exceed $3.7 \times 10^7 \text{ cm}^{-2}$. One can notice that the majority of dislocations in the InN layer propagated from the GaN buffer layer that was grown on Al_2O_3 with a large lattice mismatch. However, there are areas in the N-polar sample where vertical voids were formed. Some voids started from the interface with GaN and others were formed within the layer (not shown here for a lack of space).

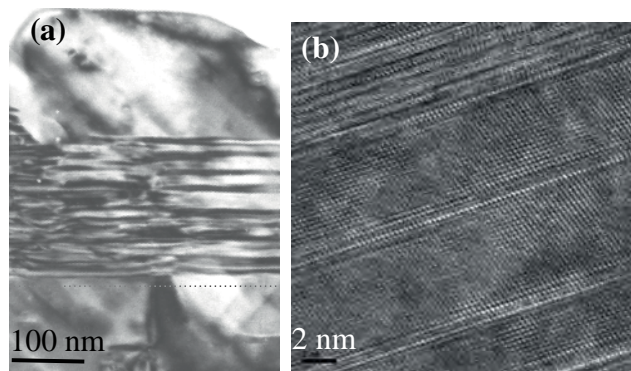


Figure 2 (a) A band of planar defects formed in the subsurface area in the sample that started to grow with In polarity and transferred to N polarity above a zig-zag inversion boundary; (b) high resolution image from this band of faults. Note a large thickness of a cubic (3C) material.

On the same figure one can see some imbedded domains with a different diffraction contrast (marked by I in Fig.1b), most probably inversion domains or areas with a different composition. In addition to dislocations a high density of planar defects in a form of dislocation loops were formed. Many of them were lining up in the areas of the undoped spacer layers (Fig. 1b). These dislocation loops often interacted with threading dislocations leading to their lower density above the loops (see right hand side of the micrograph, Fig. 1b). Formation of these loops within the spacer layers confirms the assumption of Mg floatation to the sample surface and non-uniform distribution. In the upper part of the third layer where Mg concentration reached $2.9 \times 10^{19} \text{ cm}^{-3}$ (where the change of growth polarity took place in the previous sample) many planar defects almost equally spaced (Fig. 3) are formed. With a further increase of Mg concentration to $1.8 \times 10^{20} \text{ cm}^{-3}$ a density of planar defects becomes more irregular, but at a distance of about 400nm from the surface a band of densely distributed planar defects appear again similar to that observed in the previous sample (as presented in Fig. 2). A lattice image from this area with planar defects appearing close to the sample surface show formation of dif-

ferent thicknesses of cubic material, meaning a different types of stacking fault. However, in many places the thickness of a cubic layer is much larger than required for the formation of any type of stacking fault (I_1 , I_2 or E), typical for 2H material [16]. Some top areas of the sample are completely converted to cubic material and twin defects typical for a cubic material are observed (see top center part of Fig. 1b). In the majority of areas the subsurface areas still show 2H structure.

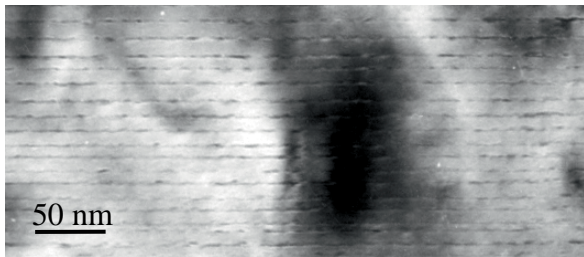


Figure 3 Stacking faults almost equally distributed in the sample grown with N-polarity.

As shown earlier [8] for this high Mg concentration ($>1.8 \times 10^{20} \text{ cm}^{-3}$), a change from p-conductivity to n-conductivity is taking place in both samples that started to grow with a different polarities. For the same Mg concentration a band of planar defects is formed. It is worth noting that these defects appear always in N-polar material since a change of polarity took place in the sample that has started to grow with In-growth polarity.

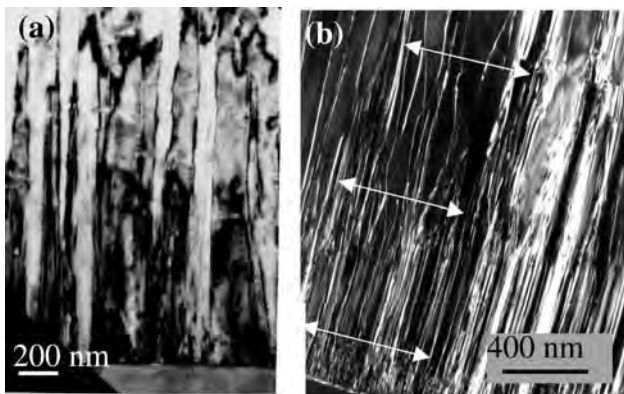


Figure 4 Dislocation distribution in a sample grown with constant In polarity (a) and a constant N polarity (b). The arrows indicate areas where planar defects are formed leading to dislocation interaction and decrease their density in the upper part of the layer.

For the $3 \mu\text{m}$ thick sample grown with In-growth polarity with constant Mg concentration of $6 \times 10^{18} \text{ cm}^{-3}$, the density of dislocations is rather high and reaches $1.6 \times 10^{10} \text{ cm}^{-2}$ (Fig. 4a). They are of edge type and their density does not decrease with sample thickness. This is in agreement with our earlier studies of the thick In-polar samples grown in a

different laboratory with Mg concentration below 10^{19} cm^{-3} [10].

The $7.3 \mu\text{m}$ thick sample grown with N-growth polarity with constant Mg concentration of $3 \times 10^{19} \text{ cm}^{-3}$ is the most structurally poor sample among four samples studied. The density of dislocations at the area close to the interface with GaN is about $1 \times 10^{11} \text{ cm}^{-2}$ and slightly decreases toward the sample thickness (Fig. 4b). These decrease is caused by the formation of planar defects (indicated by arrows) at a discrete distances from the interface such as $0.4 \mu\text{m}$, $1.2 \mu\text{m}$ interface and $\sim 3 \mu\text{m}$ suggesting again Mg floating to the growth surface. Due to the formation of the planar defects dislocation density decreases to $2 \times 10^9 \text{ cm}^{-2}$ in the subsurface area.

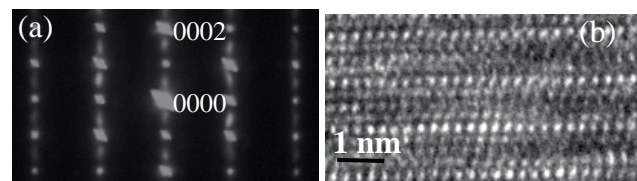


Figure 5 (a) A selective area diffraction pattern (SAD) indicating division of the 0002 distance into four indicating some ordering consistent with 4H polytype structure; (b) High resolution lattice image from the same area.

In few areas of this particular sample selective area diffraction (SAD) patterns showed additional spots dividing 0002 distance into four (Fig. 5a). High resolution images show that each fourth 0002 lattice fringe has higher intensity and a specific lattice arrangement suggesting some ordering consistent with the formation of 4H polytype (Fig. 5b). The reason for the formation of such a polytype is not clear since in some areas of the sample this polytype starts from a non-uniform interface, but with an abrupt and uniform interface this polytype starts from a band of planar defects, mentioned above, located at some distance from the interface. This 4H polytype might extend to another band of planar defects, formed for different sample thickness, converting again to 2H InN at the surface. To our knowledge this is the first experimental observation of the 4H type of polytype in this type of samples.

These studies show that type of defects formed in the InN:Mg depends strongly on growth polarity. Samples that grow with N polarity are more susceptible to the formation of planar defects than these grown with In polarity. Two other structures besides 2H have been observed: 3C and 4H structure found in this study.

4 Discussion and conclusion The addition of Mg to InN leads to the formation of different types of structural defects. The type of defect depends on sample growth polarity. In the samples grown with N-polarity for Mg concentration $>10^{19} \text{ cm}^{-3}$, equally spaced stacking faults are formed in 2H structure. For the higher concentration $>10^{20} \text{ cm}^{-3}$, a band of planar defects with a large thickness of a cubic material can be observed in the sub-surface area. For the thick samples with a constant Mg concentration of

$3 \times 10^{19} \text{ cm}^{-3}$, the 4H polytype could be found in some areas of the sample. The question remains what leads to this behavior. Is it a Mg a leading factor or the fact that we are dealing at least with three elements with different radii? There are many Mg rich ternaries like $\text{Zn}_{1-x}\text{Mg}_x\text{Se}$ [17] or $\text{Cd}_{1-x}\text{Mg}_x\text{Te}$ [18] with these type of defects and polytypes but there are also other materials like $\text{Zn}_{1-x}\text{Cd}_x\text{S}$ and $\text{ZnS}_{1-x}\text{Se}_x$ [19], or SiC [20] with different dopants where polytypes are also often observed. The observation of densely distributed stacking faults in InGaN and large areas of cubic materials with either high In content or large sample thickness [21] and InGaN:Mg [22] would suggest that different atomic radii might be the reason for the formation of different polytypes. This is an important issue since change of polytypes from 3C \rightarrow 8H \rightarrow 4H \rightarrow 2H in ZnMgSe [17] leads to a change of a bandgap from 2.94 eV to 3.08 eV, an important issue for III-Nitrides. This would shed a light that a previous dispute of a different value of a bandgap in InN most probably was related to structural variety of the samples grown in different laboratories.

In conclusion, one can see that In-polar samples change growth polarity to N when Mg concentration is exceeding a specific concentration of few times 10^{19} cm^{-3} . In contrast, N-polar samples do not change growth polarity for the same Mg concentration. However, they are more vulnerable to the formation of different types of planar defects (stacking faults and dislocation loops) and also to the formation of different polytypes. In these N-polar samples there are several areas where planar defects interact with dislocations decreasing in this way their density. For both starting growth polarities a band of planar defects with extended layers of cubic material (defective polytypes) is formed when the Mg concentration exceeds $1.8 \times 10^{20} \text{ cm}^{-3}$. The presence of this band of defects with a large thickness of cubic material might be responsible for n-type conductivity reported earlier [8] for heavily Mg-doped films, since layers with lower Mg concentration, where these defects were not observed, show p-conductivity.

Acknowledgements This work was supported by the Director, Office of Science, Office of Basic Energy Sciences, Materials Sciences and Engineering Division, of the U.S. Department of Energy under Contract No. DE-AC02-05CH11231. All studied samples were grown at Chiba University, Chiba, Japan. The use of the facility of the National Center for Electron Microscopy in LBNL, Berkeley is appreciated.

References

- [1] V.Y. Davydov, A.A. Klochikhin, R.P. Seisyan, V.V. Emtsev, S.V. Ivanov, F. Bechstedt, J. Furthmüller, H. Harima, A.V. Mudryi, J. Aderhold, O. Semchnova, and J. Graul, *Phys. Status Solidi B* **229**, R1-R3 (2002).
- [2] J. Wu, W. Walukiewicz, K.M. Yu, J.W. Ager III, E.E. Haller, H. Lu, W.J. Schaff, Y. Saito, and Y. Nanishi, *Appl. Phys. Lett.* **80**, 3967-3969 (2002).
- [3] A.V. Blant, T.S. Cheng, N.J. Jeffs, L.B. Flannery, I. Harrison, J.F.W. Mosselmanns, A.D. Smith, and C.T. Foxon, *Mater. Sci. Eng. B* **59**, 218-221 (1999).
- [4] V.V. Mamutin, V.A. Vekshin, V.Y. Davydov, V.V. Ratinikov, Y.A. Kudriavtsev, B.Y. Ber, V.V. Emtsev, and S.V. Ivanov, *Phys. Status Solidi A* **176**, 373-378 (1999).
- [5] W. Walukiewicz, *Physica B* **302**, 123-134 (2001).
- [6] H. Lu, W.J. Schaff, L.F. Eastman, and C.E. Stutz, *Appl. Phys. Lett.* **82**, 1736-1738 (2003).
- [7] S.X. Li, K.M. Yu, J. Wu, R.E. Jones, W. Walukiewicz, J.W. Ager III, W. Shan, E.E. Haller, H. Lu, and W.J. Schaff, *Phys. Rev. B* **71**, 161201 (2005).
- [8] X. Wang, S. B. Che, Y. Ishitani, and A. Yoshikawa, *Appl. Phys. Lett.* **91**, 242111 (2007).
- [9] X. Wang, S. B. Che, Y. Ishitani, and A. Yoshikawa, *Appl. Phys. Lett.* **91**, 081912 (2007).
- [10] Z. Liliental-Weber, in: *Indium Nitride and Related Alloys*, edited by T.D. Veal, C.F. McConville, and W.J. Schaff (CRS Press Taylor & Francis Group, Boca Raton, London, New York, 2008), pp. 515-540.
- [11] Y. Nanishi, T. Araki, and T. Yamaguchi, in: *Indium Nitride and Related Alloys*, edited by T.D. Veal, C.F. McConville, and W.J. Schaff (CRS Press Taylor & Francis Group, Boca Raton, London, New York, 2008), pp. 1-50.
- [12] T.L. Tansley and C.P. Foley, *J. Appl. Phys.* **59**, 3241-3244 (1986).
- [13] X. Wang, S.B. Che, Y. Ishitani, and A. Yoshikawa, *J. Appl. Phys. Part 2* **45**, L730 (2006).
- [14] X. Wang, S.B. Che, Y. Ishitani, and A. Yoshikawa, *J. Appl. Phys.* **99**, 073512 (2006).
- [15] L. Romano, J.E. Northrup, A.J. Ptak, and T.H. Myers, *Appl. Phys. Lett.* **77**, 2479 (2000).
- [16] D. Hull and D.J. Bacon, in: *Introduction to Dislocations*, 3rd ed., Internat. Series on Materials Science and Technology, Vol. 37 (1985), pp. 112-121.
- [17] W. Paszkowicz, P. Dluzewski, Z.M. Spolnik, F. Firszt, and H. Meczynska, *J. Alloys Compd.* **286**, 224 (1999).
- [18] E. Michalski, M. Demianiuk, S. Kaczmarek, and J. Zmija, *Acta Phys. Polon. A* **56**, 333 (1979).
- [19] M. J. Kozlowski, *J. Cryst. Growth* **30**, (1975) 86.
- [20] J.F. Kelly, G.R. Fisher, and P. Barnes, *Mater. Res. Bull.* **40**, 249 (2005).
- [21] Z. Liliental-Weber, K.M. Yu, M. Hawkrige, S. Bedair, A.E. Berman, A. Emara, J. Domagala, and J. Bak-Misiuk, *Phys. Status Solidi C* **6**(S2), S433 (2009).
- [22] M. E. Hawkrige, Z. Liliental-Weber, K. M. Yu, L. A. Reichertz, W.J. Schaff, J. W. Ager, and W. Walukiewicz, *Phys. Status Solidi C* **6**(S2), S421 (2009).